ENAC – Faculté environnement naturel, architectural et construit

MCS MAINTENANCE CONSTRUCTION SÉCURITÉ
INSTITUT D'INGÉNIERIE CIVILE

ÉCOLE POLYTECHNIQUE FÉDÉRALE DE LAUSANNE

Soft load testing and associated deck slab monitoring of Morges A1 highway bridge, Switzerland

MCS Test Report number 23.13.03

Mark A. Treacy BE MSc CEng

Prof. Dr. Eugen Brühwiler, ing. civil dipl. EPFZ/SIA

In the framework of the TEAM project, a Marie Curie Initial Training Network, funded by the European Commission FP7 Programme (PITN-GA-2009-238648).

TRAINING in EUROPEAN ASSET MANAGEMENT
TEAM

Lausanne, 27 March 2014

Adresse postale : EPFL ENAC IS MCS, GC B2 402 (Building GC), Station 18, CH-1015 Lausanne /

tél: +41 (0)21.693.28.85 fax:+41 (0)21.693.58.85 http://mcs.epfl.ch

This page is intentionally left blank.

Contents

1 Introduction

1.1 Context and motivation

A technical challenge in the management of road bridge stocks is obtaining a reliable estimate of the remaining service life in order to efficiently plan and coordinate replacement or improvement interventions. In the past, fatigue of reinforced concrete (RC) has not been the limiting factor to service life; with concrete degradation, reinforcement corrosion or insufficient load capacity often the primary reasons for interventions. With recent improvements in durability approaches to materials and proactive maintenance strategies, high-cycle fatigue requires increased consideration in RC or prestressed concrete road bridges.

Efficient safety verification techniques are therefore required in order to avoid unnecessary interventions and identify potential problems well in advance. A substantial research base now makes it possible to examine the load carrying capacity of most road bridges with reasonably accuracy. The greater source of uncertainty lies on the traffic loading or, more specifically, the action effects at the element level.

The advent of cheap and high storage capacity hardware in recent years means direct measurement of elemental action effects via structural monitoring is now a viable option. Monitoring can overcome limitations of accurately modelling in-service behaviour at an elemental level. For example, material properties change over time and secondary elements such as parapets, kerbs and surfacing layers reduce the stress levels in the steel reinforcement bars (rebars). This can provide uncertainty in modelling but these effects are inherent in the measured data. These reasons can justify the use of a monitoring regime for the accurate determination of real ‘action effects’ to demonstrate strength reserves not captured using traditional codified approaches.

1.2 Approach

This project involves the monitoring of a busy 1960’s highway bridge within the Swiss road network. A monitoring system was installed in the bridge during August / September 2011. The system measures multiple phenomena at strategic locations using a various sensors giving a ‘Smart Section’ from which the results can be used to improve structural models and better understand the traffic action behaviour. The emphasis is on the action effects arriving in the reinforcement bars (rebars) of the deck slab with a key focus being the direct measurement of strains in the transverse reinforcement of the girder’s top flange.

1.3 Objectives

1.1 Overall project objectives

The goal of particular study is to test the monitoring system after its installation. This report presents a series of ‘soft load tests’ tests carried out on the morning of November 6th 2011 with a crane of approximately 60 tonnes.

Long term objectives of the project will be to investigate if fatigue is ever a risk for rebars of such deck slabs. This will be addressed by performing long-term high-frequency monitoring of the slab for over one year. Secondly, the question “what are the extreme characteristics of the measured action effects in the long-term?” will be addressed which is vital for planning future monitoring projects.

1.2 Specific objectives of this report

The overall aim of this report is to describe the bridge monitoring system and present the results of soft load tests performed with an extreme vehicle of almost 60 tonnes after installation of the monitoring system. This would confirm if the system is operating correctly and if it can adequately capture such events. This vehicle is almost 20 tonnes greater than the normal legal limit for trucks in Switzerland and required special permission from the road authorities and a police escort. The aim was to produce a measurable response in the bridge elements which should be captured by the monitoring system. The data will be subsequently analysed to ensure the monitoring system is performing correctly.

Due to the nature and strategic importance of this highway a full road closure was impossible for the test therefore a 'soft loading' approach was chosen using heavy traffic as the test load. The term 'soft load test' is used as the actual traffic on the bridge is used as the loading source without a requirement to close the road. Soft load testing is not intended to predict the ultimate state behaviour of a bridge but rather to optimise its structural model used for safety assessment under serviceability conditions [1]. The test was carried out at a time when there are very few vehicles on the bridge, mainly family cars which would not interfere significantly with the results.

1.4 Scope of report

This study at present is limited to the bending effects of the deck slab from test measurements on Sunday November 6th 2011. The overall longitudinal bending effects in the girder such as the strain in the prestressing tendons have not been examined in this work. The report is limited to explanation of the monitoring system and this single day's test series, and the interpretation of local sensor measurements. This is not a full structural safety verification of the bridge.

When carrying a soft load test, it is generally recommended that the measurements should acquire at least 100 relevant (loaded) trucks heavy vehicles in each lane are recorded for reliable calculation of influence lines and of load distribution factors [2]. This would normally be the case for specific bridge assessments where there exists a known problem. In this case the data is required for research purposed and the budget available meant a smaller number of individual runs of a single extremely heavy vehicle were possible. The data recorded is not required to estimate vehicle weights (as a B-WIM system) but rather to study and characterise the action effect behaviour.

2 Description of bridge and location

The monitored bridge was constructed around 1963 and is located on Swiss A1 highway between Geneva and Lausanne adjacent to the train station at Morges, Vaud. The structure consists of twin prestressed box girders of three spans of 35 m, 39 m and 35 m with a total length of 110.5 m (Figs. 1/2). The bridge is split into two nearly identical, structurally independent, girders of 11.47 m width. The end supports are both pin-jointed and rest on reinforced concrete (RC) abutment walls supported on RC spread footings, while the interior columns are supported by pad foundations.

(a) (b)

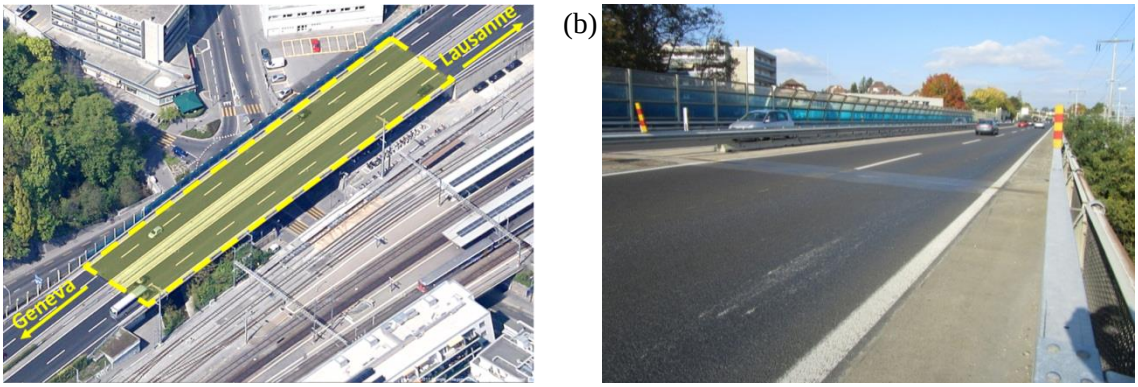

Figure 1. (a) Aerial view of bridge adjacent to Morges train station (www.googlemaps.com) and; (b) View towards Lausanne showing thermal expansion joint (Geneva end).

Information on the geometry and the construction of the bridge was obtained from original design documents and a technical bulletin from that time [2]. The annual average daily traffic (AADT) volumes are in the region of 70 000 vehicles [3]. In addition to the longitudinal prestressing, the girders are also transversely prestressed in the upper deck slab.

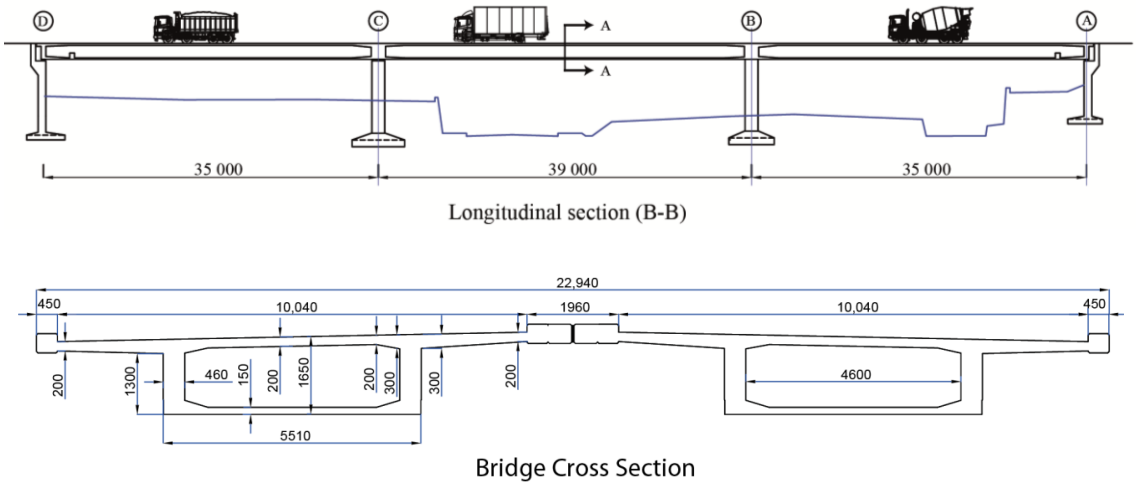

Figure 2. Side Elevation and Cross-section showing principal dimensions (in mm).

Originally, both of the end supports were twin neoprene sliding joints to allow for some vertical and horizontal movement caused by thermal expansion. Figure 3 illustrates the structural degrees of freedom available at each of the supports.

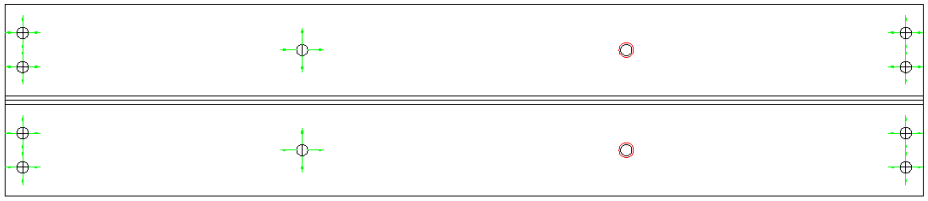

Figure 3. Schematic of the original support conditions.

In later works in 1986, additional restraints were added at both ends to prevent transverse movement which can be seen in the middle of the Figure 4.

Figure 4. End Support showing additional lateral fixities in centre (Geneva end).

Each girder has 1.35 m diameter intermediate columns as the inner supports with one of them fully fixed and the other vertically restrained only as shown in Figure 5. The internal column on the Geneva side is fixed (Fig. 5(a)).

(a)  (b) 

Figure 5. (a) Column fixed Support and; (b) Column Roller support.

3 Monitoring system

The centre of the inner span was selected for the Smart Section (Fig. 6) as it provides good information on both the lateral and transverse behaviour. As the two girders in each direction are completely identical but separated structures only one girder was instrumented for this study. The system was installed over a number of visits to the bridge in July and August 2011. The system is fully accessible remotely via a wireless internet connection within the bridge allowing constant access for data transfer and modification of the measurement programme. Additional details on the bridge monitoring system are contained in [4].

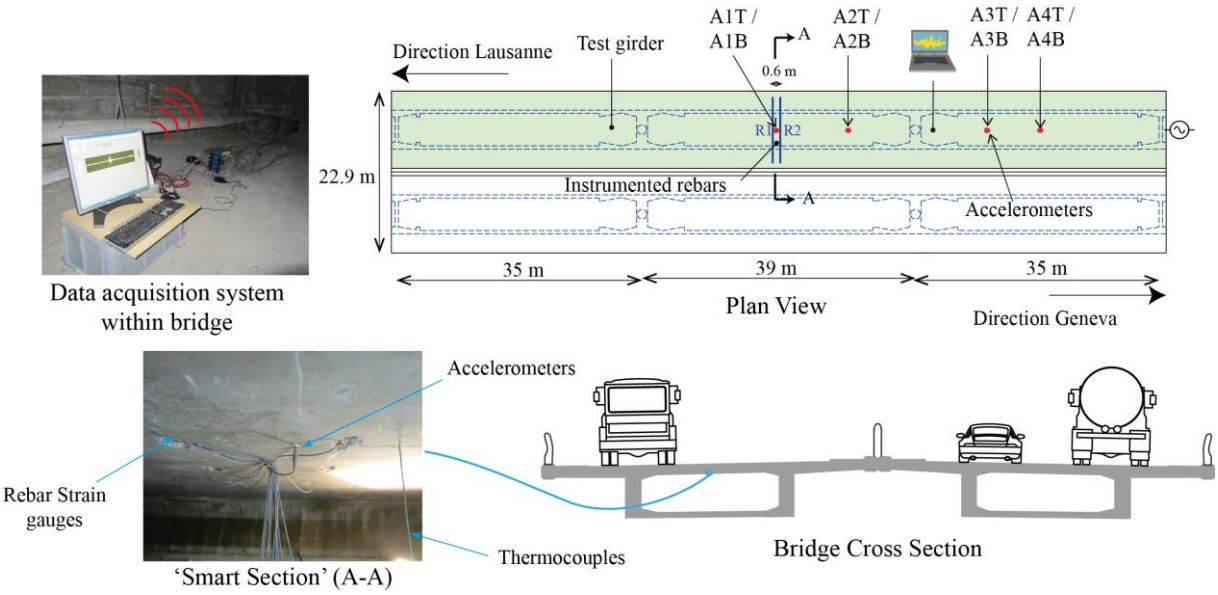

Figure 6. Schematic of the bridge monitoring system.

The monitoring system contained the following equipment with further technical details for the sensors given in Annex D:

- PC within the box girder: Apple Mac Mini with 200 GB storage capacity and Intel R core.
- 3 HBM QuantumX MX840A data receivers for measurement of strains and accelerations.
- 1 HBM QuantummX MX1609 data receiver for measurement of temperature.
- 1 QuantumX CX27
- Strain gauges on reinforcement type HBM 1-LY61-3/120.
- Strain gauges on the concrete structure type HBM LY41-100/120 with temperature compensation adaptors.
- Uniaxial accelerometers type HBM 1-B-12/200.
- Globesurfer III wireless internet router.

Accelerometers were used for the characterisation and monitoring of the bridge's global dynamic behaviour and to assist decision making on sampling rates for strain gauge monitoring. Eight accelerometers were placed on the bridge at four locations (Fig. 6). At these locations one accelerometer was fixed to the top of the lower flange and one to the underside of the upper flange.

The installation of strain gauges on rebar required the local removal of cover concrete in the region of the proposed sensors. In order to limit damage to the concrete structure to an absolute minimum, GPR (ground-penetrating radar) techniques were used to locate the reinforcement bars to be instrumented (Fig. 7).

Figure 7. Locating rebars using a GPR system.

Two 10 mm diameter transverse rebars and two 12 mm rebars in the longitudinal direction were each instrumented with electrical resistance strain gauges (Fig. 8). The arrangements feature half bridge configurations incorporating compensation strain gauges on steel plates to avoid problems with temperature drift. Additional discussion on removing long-term thermal effects is provided in [6]. As the study is concerned with live load or traffic induced stress cycles the gauges can be zeroed each morning so long term drift is not a problem. This means the results are reference free but the inherent self-weight stresses in the elements are not of interest in this particular case. Photos of all the rebar strain gauges are contained in Appendix A.

(a)

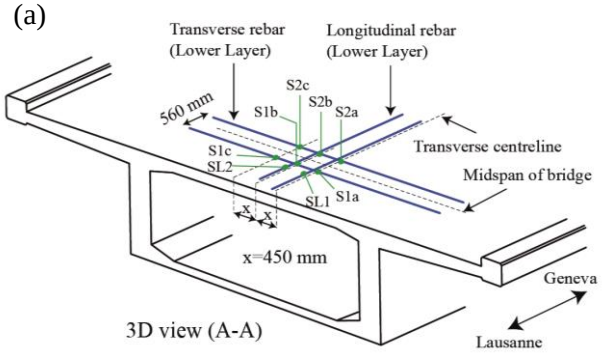

(b)

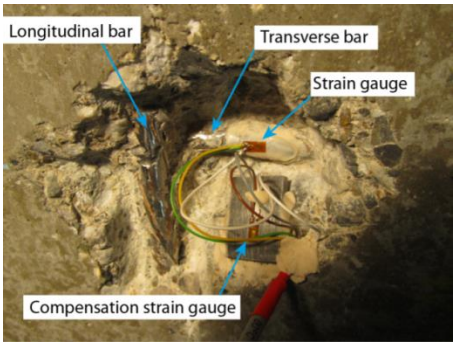

Figure 8. (a) 3D view of strain gauge locations on rebars and; (b) Strain gauges on a transverse rebar with local temperature compensation.

The positions of the accelerometers and concrete strain gauges on the Smart Section are illustrated in Figure 9(a). In order to examine the thermal effects on the measured action effects a series of thermocouples are also included on the same cross section (Fig. 9(a)). They were drilled 30 mm into the concrete. Air temperature and relative humidity were also recorded inside the girder using a separate system. The two-dimensional stress state in the slab can be examined by providing pairs of 10 cm long strain gauges on the concrete structure in two orthogonal directions as shown in Figures 9(b) and 10. Note the LSG and TRS sensors are shown in Figure 10 as C1 to C8.

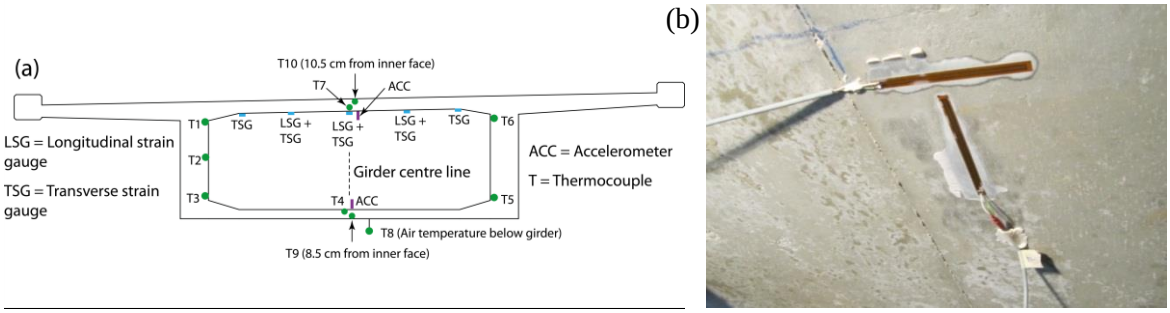

Figure 9. (a) Locations of sensors on Smart Section and; (b) 10 cm strain gauges glued directly on the uncracked concrete.

The exact positioning of the strain gauges on the reinforcement and concrete structure on the underside of the deck slab are illustrated in Figure 10. Only the four rebars of interest are shown for clarity but a detailed reinforcement drawing of the cross-section is contained in Appendix C.

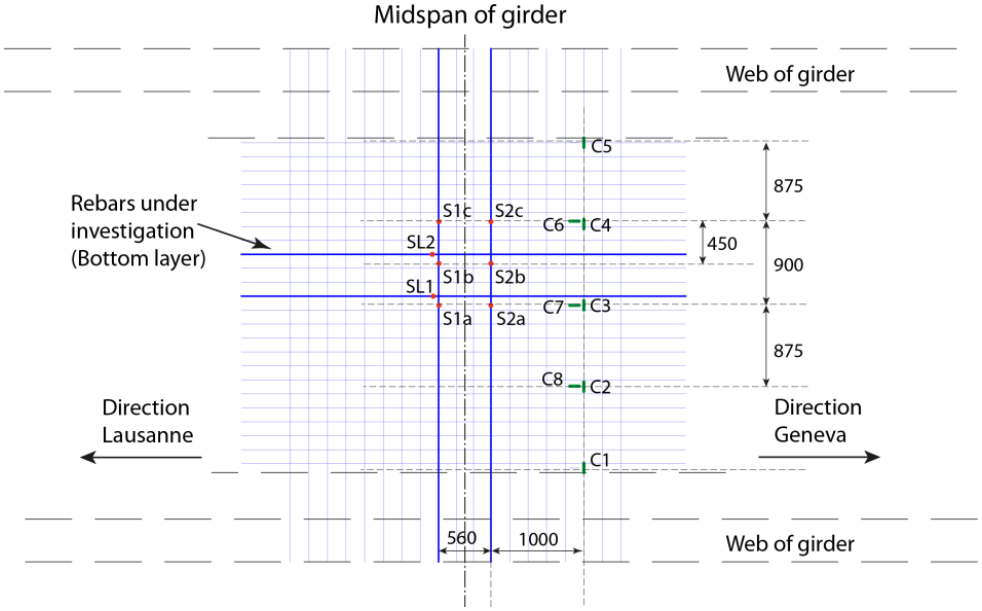

Figure 10. Location of Smart Section strain gauges on underside of deck slab.

Once operational, all of the measurable parameters can be viewed on the control panel display of the monitoring software as demonstrated in Figure 11. An interface for the monitoring system was written in the Lab View software allowing alteration to monitoring regimes and providing ‘on line’ visualisation of data being recorded.

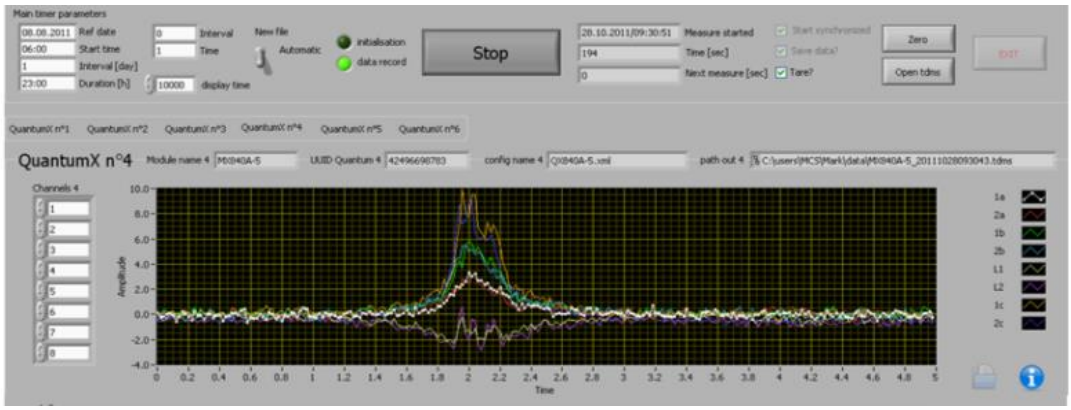

Figure 11. Screenshot of monitoring Lab View interface showing the live response due to a truck as strain in reinforcement bars.

In this test series the sampling rate for all strain gauges and accelerometers was 200 Hz with a Bessel low pass filter applied to remove any high frequency interference. The thermocouple data was recorded with a sampling rate of 1 Hz. Note the sampling rates were subsequently reduced for later tests as described in [6].

4 Test Vehicle

The vehicle used in the tests was a GMK 5130-2 mobile crane as shown in Figure 12. The vehicle was weighed statically at a weigh station before the test and a gross weight 58.75 tonnes (576.3 kN) was found. Each axle load is just below the legal limit of 12 tonnes for road vehicles in Switzerland. The tyres are of the type 14.00 R with a nominal pressure of 10 bar.

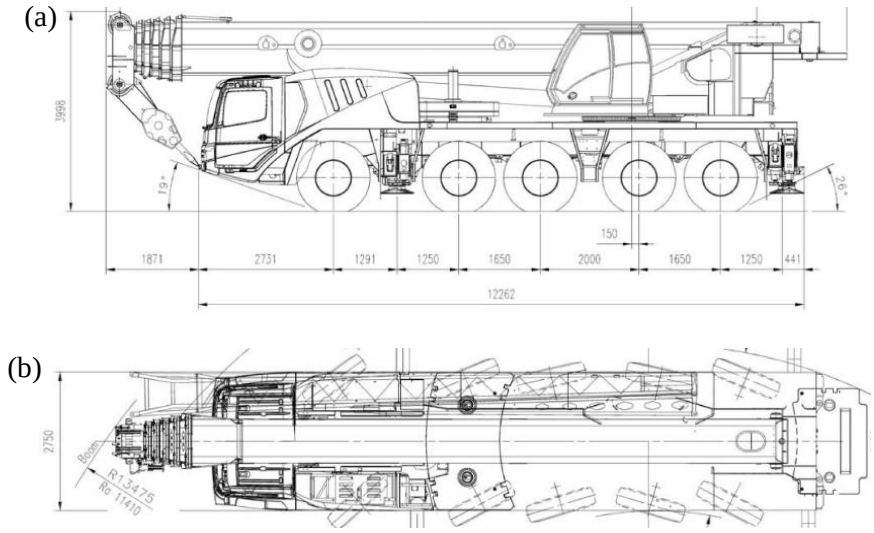

Figure 12. (a) Side elevation of test vehicle and; (b) plan view of test vehicle.

5 Test Details

The test series involved the vehicle performing loops along the A1 highway between Crissier and Morges West. For the higher speed tests the vehicle exited at Bussigny instead of Morges West in order to have a longer stretch of road to reach the required velocity. All of the tests were filmed with digital camera located before the Geneva end of the bridge as shown in Figure 13(a). A video file of the tests has also been complied.

Figure 13. Location of video camera.

The lateral position 'Y' of the vehicle, required for later numerical simulations, is referenced from the south-west corner of the bridge which is chosen as the origin as shown in Figure 14.

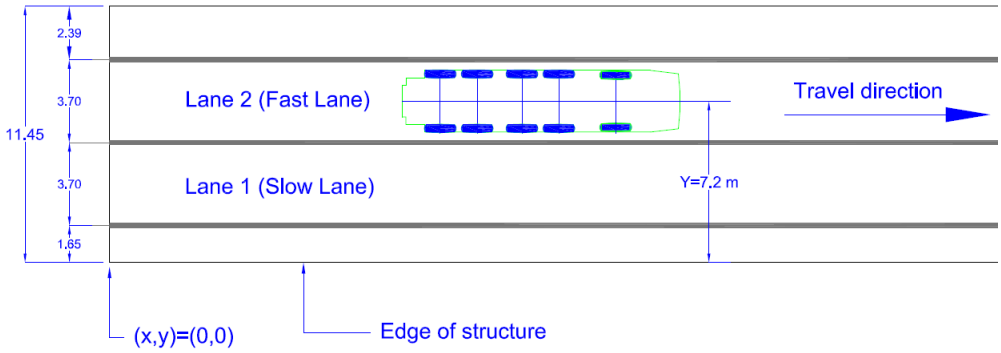

Figure 14. Arrangement of lanes and vehicle positioning notation.

Nine separate test runs over the bridge were carried out between 07:41 and 10:15 (with low volumes of car traffic) and, each time the vehicle crossed the bridge, the lateral position and velocity were varied as recorded in Table 1.

Table 1. Summary of test variables.

Test Number	Lane	Velocity (km/h)	Arrival time	Lateral position (m)
1	Fast	85	07:41	1.85
2	Fast	45	07:56	1.85
3	Slow	85	08:22	1.85
4	Slow	45	08:39	1.85
5	Slow	40	08:57	0.95
6	Slow	40	09:15	0.85
7	Fast	85	09:42	1.75
8	Slow	40	09:58	1.75
9	Slow	35	10:15	0.85

The weather conditions on the day of the test were dry and calm. The air temperature during the tests is shown in Figure 15(a) while the concrete temperature at various points on the inside of the girder during the test is shown in Figure 15(b).

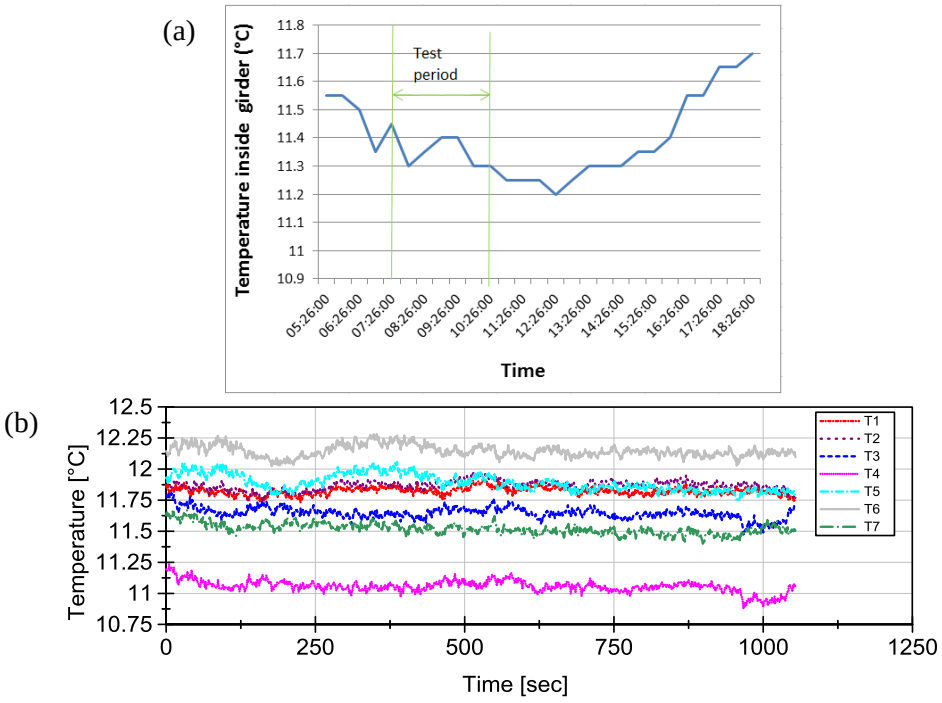

Figure 15. (a) Air temperature within the end-span (Geneva side) of the girder and; (b) Temperatures around girder cross section during Test 1.

6 Results and discussion

This section presents the results from strain gauges on the steel rebars and concrete structure. It was possible to capture the vehicle passage during each of the nine tests. The raw measured strain signals are generally offset from the x-axis as the system does not automatically zero the system. Therefore, the signals are subsequently shifted to the x-axis during data treatment by subtracting the average of the first 100 non-loaded (no truck on bridge) data points. The full series of test result plots is contained in Appendix B.

6.1 Strain in steel reinforcement bars

Confidence in the system was assured by comparing the behaviour of sensors at the same lateral position on different bars. i.e. S1a/S2a, S1b/S2b, S1c/S2c and SL1/SL2. Figure 16 shows the results from the strain gauges on the rebars during test 3. The signature of each of the crane's five axles can be clearly seen in each sensor with a slight time lag between the corresponding sensors on the two bars to account for the time taken for the vehicle to pass from one to the other. I.e. the vehicle passed over rebar 2 first therefore reading S2a is offset slightly to the left hand side of reading S1a.

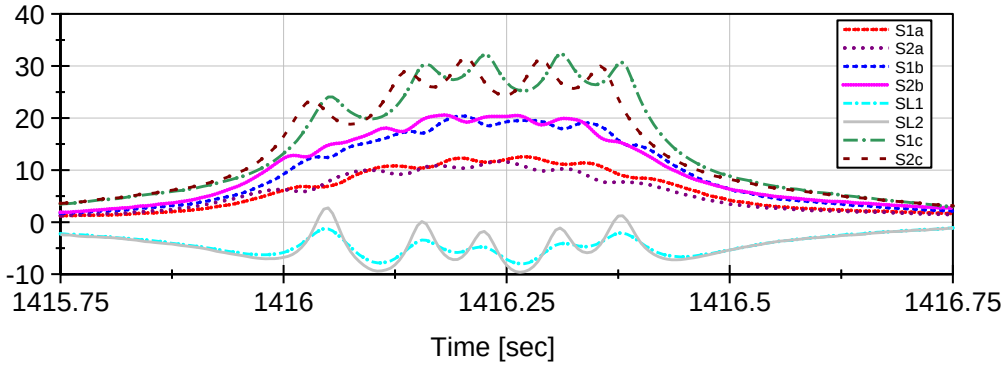

Figure 16. Strain on rebars during Test 3.

The maximum recorded strain was 74 με on gauge S1c in which is equivalent to 15.2 Mpa with a Young's Modulus value of 210 kN/mm^2 for this steel. This strain is far below any fatigue limit for steel reinforcement bars of this type and would therefore not cause any fatigue problems for the steel reinforcement at this location. Furthermore the section is compressed from the transversal prestressing of approximately 670 kN/m (assuming 10% loss in prestress since construction).

6.2 Strain on concrete structure

The effects of the five vehicle axles are also identifiable on the strain signals from the gauges on the concrete slab as shown in Figure 17. As these gauges are further away from the neutral axis than those on the steel bars the measured strain amplitudes are higher but the behaviour is very similar. These signals are observed to be much 'noisier' than the steel gauges at lower strain levels which may be due to the damping out of slab vibration and the fact that the gauge length is much longer. Results for the tests are contained in Appendix B except for tests 1 and 2 which are not plotted due to a problem with the signals from the gauges.

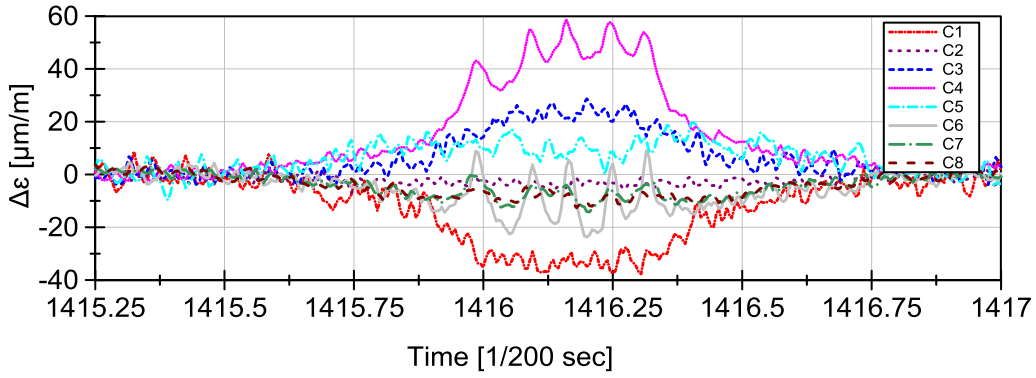

Figure 18. Strain on concrete during Test 3.

Temperature effects are not significant in the gauges on the rebars or the concrete over such a short monitoring time period but have been discussed in references [4] and [6].

6.3 Bridge dynamic behaviour

The dynamic behaviour has been examined separately in reference [4]. An FFT of the measured accelerations yields a first vertical vibration mode of approximately 2.8 Hz during tests carried out in October 2011 which is similar to other bridges of this type and geometry.

(a)

(b)

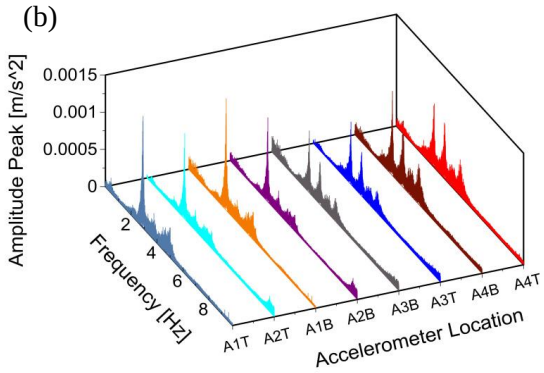

Figure 18. (a) Accelerometer on top of lower flange and; (b) Frequency spectrums of accelerometers for 1 hour measuring period for first vertical vibration mode [4].

6.4 Dynamic amplification of static load

While this number of tests is not extensive enough to have very detailed information on the dynamic amplification of vehicle loads due to higher velocities, it can be used as an indicator. Figure 19 shows little dynamic amplification of the measured strains for this particular rebar detail when the vehicle velocity is increased by a factor of two. In this case the vehicle was travelling in the slow lane.

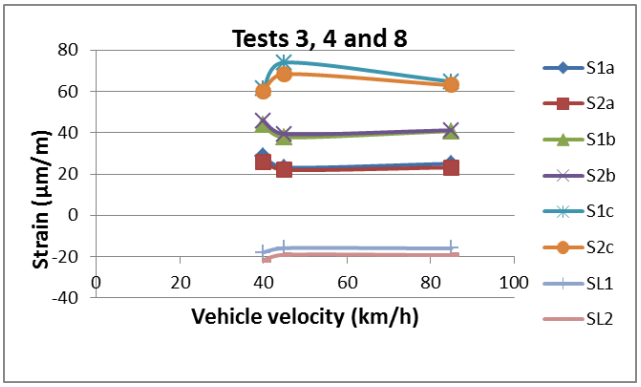

Figure 19. Strain in reinforcement bars with vehicle in centre of slow lane.

In Figure 20 for the fast lane, two of the tests provide the same measured result with almost double the velocity. Test 1 showed a higher result but this could be associated with the lateral position. I.e. the crane was not exactly on the centre of the lane as required.

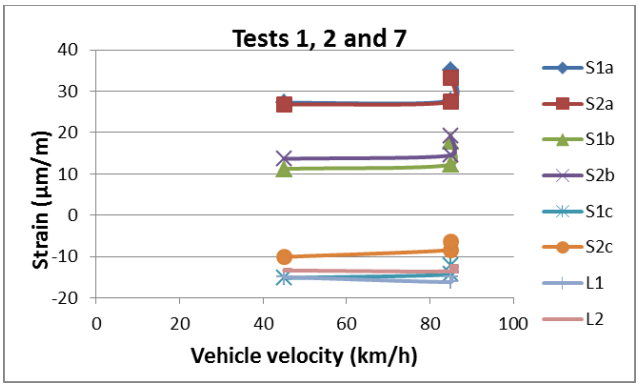

Figure 20. Strain in reinforcement bars with vehicle in centre of fast lane.

In tests 5, 6 and 9 (Fig. 21) large variation is observed for the high speed results between tests 5 and 6. The reason for the larger value in test 5 could be attributed to large variation in lateral position as the crane driver was trying to manoeuvre the truck as close as possible to the outer cantilever edge of the slow lane.

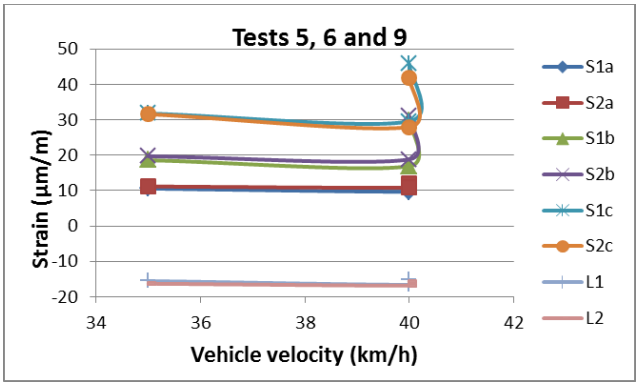

Figure 21. Strain in reinforcement bars with vehicle on exterior edge of slow lane (on side cantilever edge).

The effect of the crane on the compressive strain in the longitudinal rebars in the top flange of the girder is shown to be extremely small in Figures 20 to 22. From this limited data it seems there is no significant dynamic amplification due observable between the fast and slow velocities in this test series. Many more vehicle events would be required to provide accurate conclusions on this aspect However the result is generally in agreement with more extensive work carried out in the ARCHES project [5] where dynamic allowances close to 1.0 were found for the heavies loading scenarios on different short to medium span bridges.

7 Complimentary information

7.1 WIM measurements of test vehicle

The test vehicle crossed a nearby highway Weigh-in-Motion (WIM) station during the successive bridge tests. This system has the ability to measure the vehicle's individual loads, axle spacings, velocity and lane position. In this way the vehicle results were captured by the two separate systems. 17 passages were captured between the two WIM stations (on each highway direction) as presented in Figure 22 below. The figure shows the mean gross vehicle weight (GVW), μ, and the mean plus and minus one standard deviation, $\mu \pm \sigma$. The average error in GVW was 0.02% of the static weight for the Morges direction and 0.24% for the Lausanne direction. This is a very high level of accuracy to achieve and provides confidence in WIM data from these stations for future use in the project.

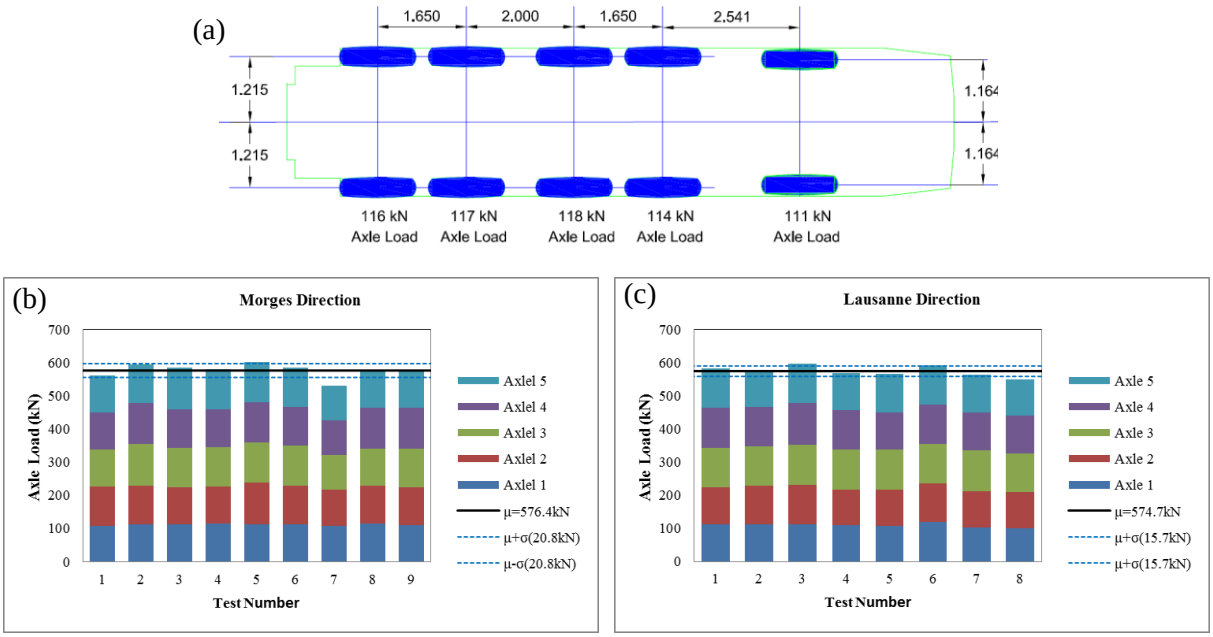

Figure 22. (a) Schematic of vehicle axle loads and; (b)/(c) Test vehicle axle load measurements through WIM stations on A1 highway at Denges, VD.

7.2 Subsequent ANSYS simulations

The calibration tests were subsequently recreated, in the finite element (FE) software ANSYS, to validate and confirm the measurements. The FE model consists of 8 noded shell elements with an apparent (to account for the steel and concrete) Young's Modulus of 45 GPa updated from static load tests. The load application area was calculated using the measured pressures of the vehicle tyres.

An example of the results for test 3 is presented in Figure 23. All of the sensor locations show a very similar overall signal shape between the measured and simulated result. The longitudinal results for sensors L1 and L2 show a strong goodness of fit providing confidence in the model globally. The transverse sensor results are reasonably close except for sensors S1c/S2c which may result from innacuracy in the assumption of wheel load spread to the neutral axis for the model. This will be investigated in further research. No allowance for dynamic amplification was applied in the structural model but the closeness in results confirms that dynamic amplification is low for extremely heavy vehicles as also demonstrated in [5].

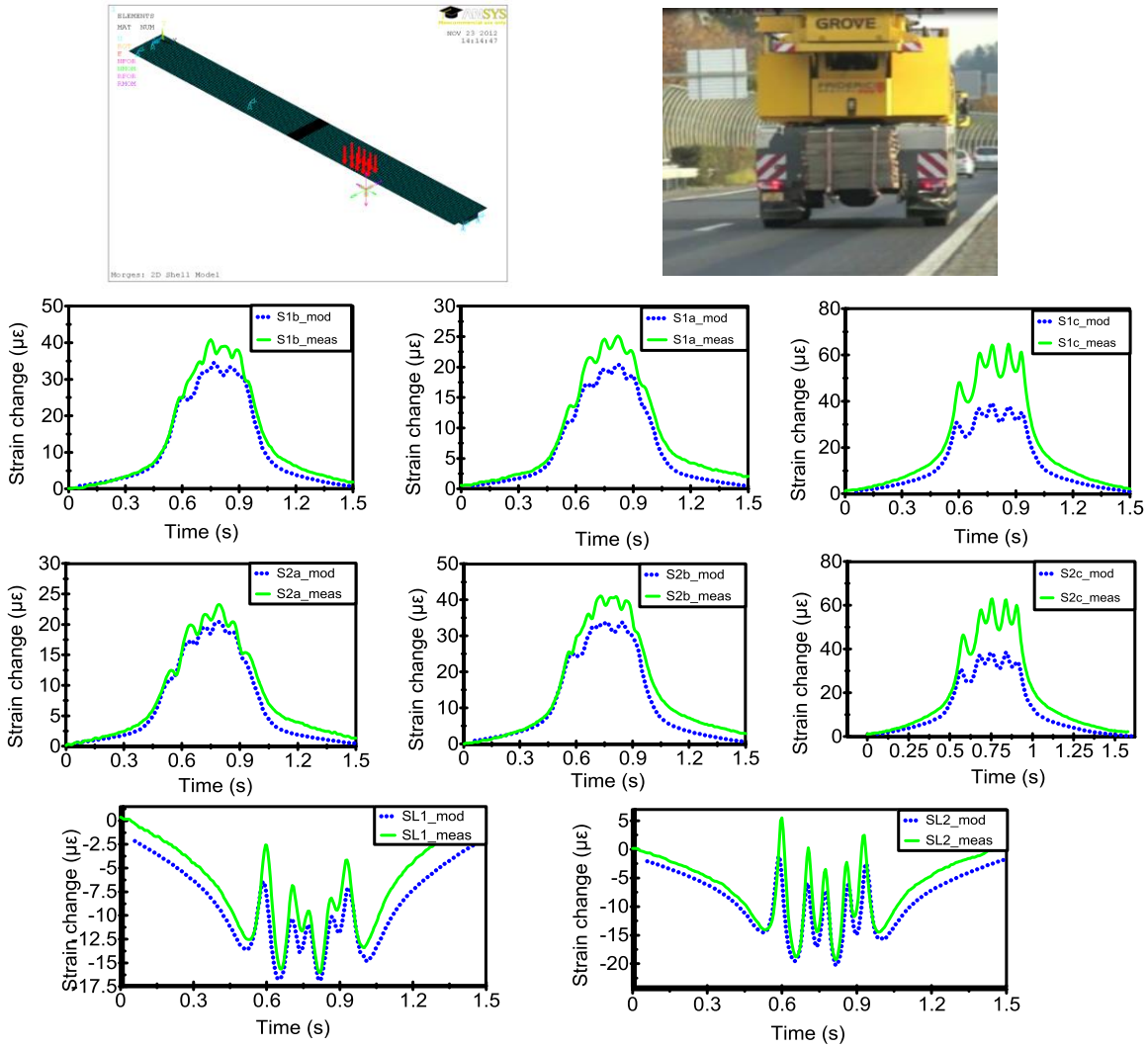

Figure 23. Comparison of ANSYS simulated (mod) and measured (meas) strain influence lines for rebars for Test 3.

8 Conclusions

This report has presented a monitoring system to measure accurately the real traffic and thermal action effects in a prestressed box girder bridge deck slab. The results of a series of soft load tests using an extreme vehicle of approximately 60 tonnes have been presented where a unique vehicle signature can be seen in the strain signals.

A number of concluding remarks on this study are as follows:

1. Direct measurement of strain in steel rebars has considerable potential as a means to assess the characteristic behaviour of extreme traffic action effects in bridge deck slabs. Measurement of the concrete structure with the chosen sensors resulted in much noisier results.
2. The five individual axles of the test vehicle are clearly identifiable from the strain signals. Excellent correlation can be seen between the corresponding gauges on the measured reinforcement bars providing confidence in the measurement system and sensor installation.
3. The chosen sampling rates and instrumentation has the ability to accurately capture the passage of a moving truck and this has been verified by a finite element comparison.
4. Dynamic amplification has been observed to be very small in the transverse direction and possibly non-existent in the longitudinal direction under the given vehicle passages but the number of passages is too little for a comprehensive study.
5. It is clear that fatigue is not a problem for the details examined in this particular bridge as the strains measured on bars and concrete far below the fatigue limit for steels, even before considering the beneficial effect of transverse prestressing.

While the elements show high margins of safety, this information can be valuable for future studies into the relationship between traffic loading and real ‘action effects’ in the structure and improvement of computer models. If the theory for calculation of the real and the beneficial contributions of surfacing, kerbs and barriers can be improved it could be applied more generally in bridges where fatigue is likely to be a problem. A continuous monitoring campaign will be carried out on the bridge for more than one year which should provide a huge level of information on the characteristics of the real bridge action effects.

Acknowledgments

The authors are grateful for the funding provided under the TEAM project, a Marie Curie Initial Training Network funded by the European Commission 7th Framework Programme (PITN-GA-2009-238648).

They would like to thank the Swiss Federal Roads Authority (FEDRO) for providing permission and access to the bridge used in this study.

Gratitude is also expressed to Gilles Guignet and Gerald Rouge of the EPFL structures lab for assistance in developing the monitoring software and installation of the sensors respectively.

9 References

[1] ARCHES Deliverable D16. 2009. Recommendations on the use of soft, diagnostic and proof load testing. Available at: http://www.arches.fehrl.org/?m=7&mode=download&id_file=9667.

[2] Bulletin technique de la Suisse romande. 1963. Le pont de la gare, à Morges, Volume 89.

[3] FEDRO. 2011 Route et traffic, chiffres et faits. Swiss Federal roads Authority, Bern. Available at: http://www.astra.admin.ch/dokumentation/00119/04504/index.html?lang=fr.

[4] Treacy M.A. & Brühwiler E. 2012. A monitoring system for determination of real deck slab behaviour in prestressed box girder bridges. IABMAS 2012 - 6th International Conference on Bridge Maintenance, Safety and Management, Politecnico di Milano, July 2012.

[5] ARCHES Deliverable D10. 2009. Recommendations on dynamic allowance. Assessment and Rehabilitation of Central European Highway Structures. Available at: http://www.fehrl.org/?m=32&mode=download&id_file=9713.

[6] Treacy M.A. & Brühwiler E. 2013. Extreme action effects in reinforced concrete bridges from monitoring. International IABSE Conference. Assessment, Upgrading and Refurbishment of Infrastructures. Rotterdam, May 2013.

Appendix A – Rebar strain gauge images

S1a (left) / SL1 (right)

S1b (left) / SL2 (right)

S1c

S2a

S2b

S2c

Appendix B – Test result plots

Test 1

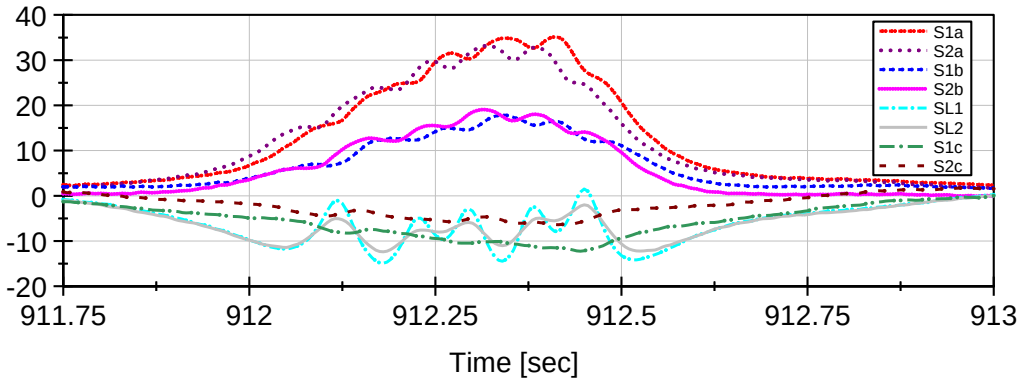

Figure B.1. Strain on rebars during Test 1.

Test 2

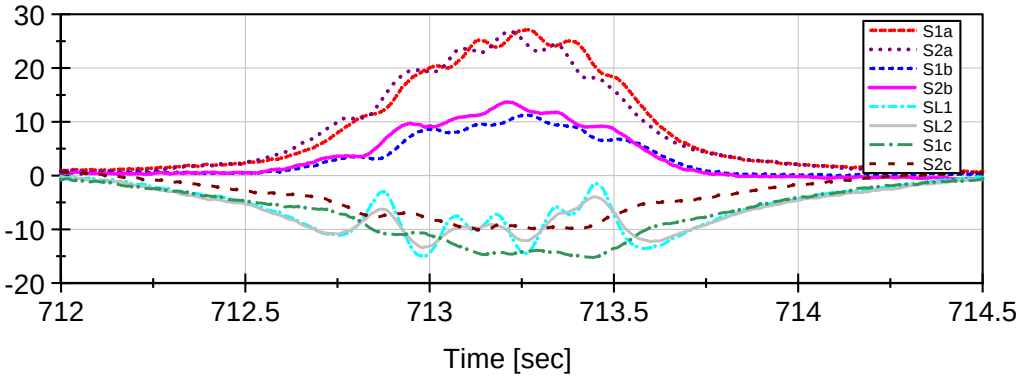

Figure B.2. Strain on rebars during Test 2.

Test 3

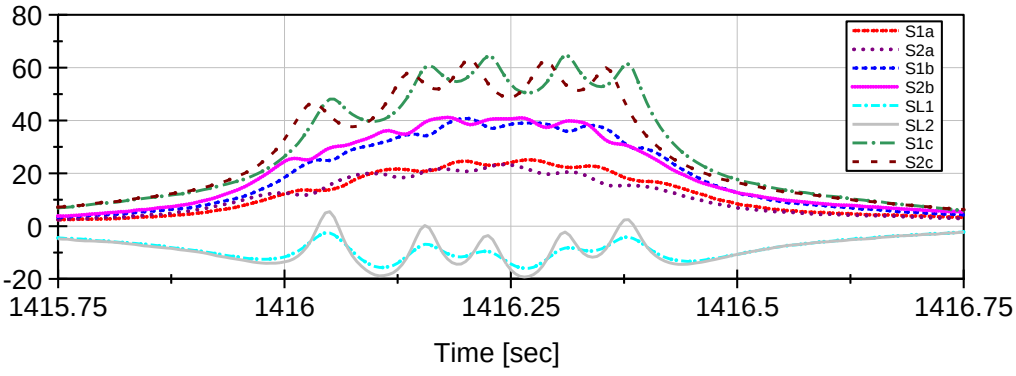

Figure B.3. Strain on rebars during Test 3.

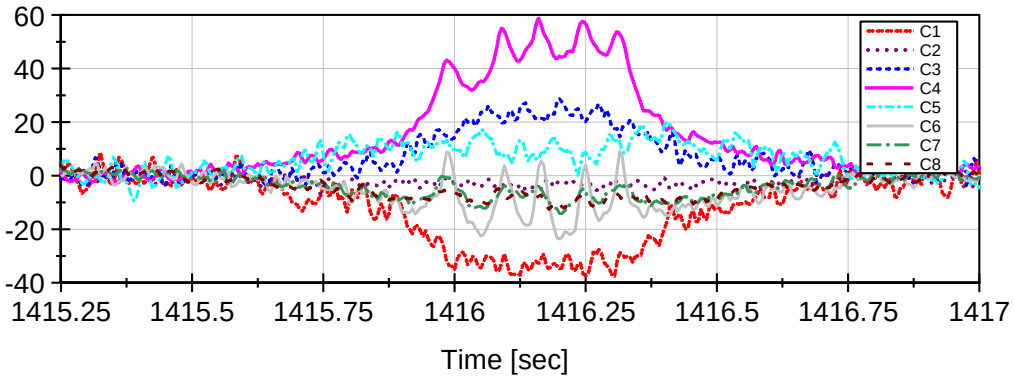

Figure B.4. Strain on concrete during Test 3.

Test 4

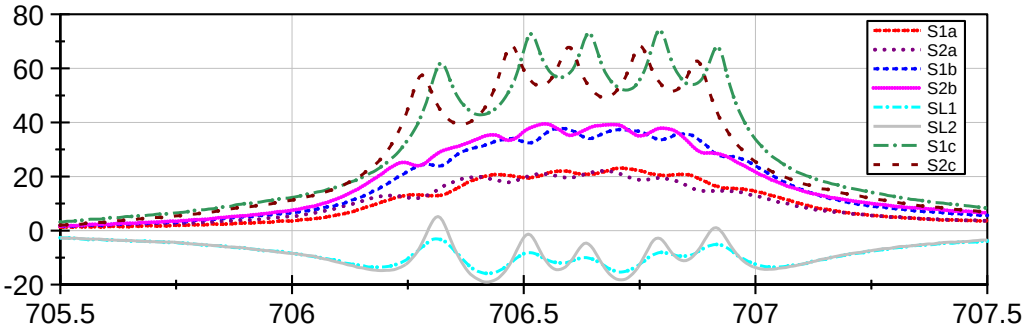

Figure B.5. Strain on rebars during Test 4

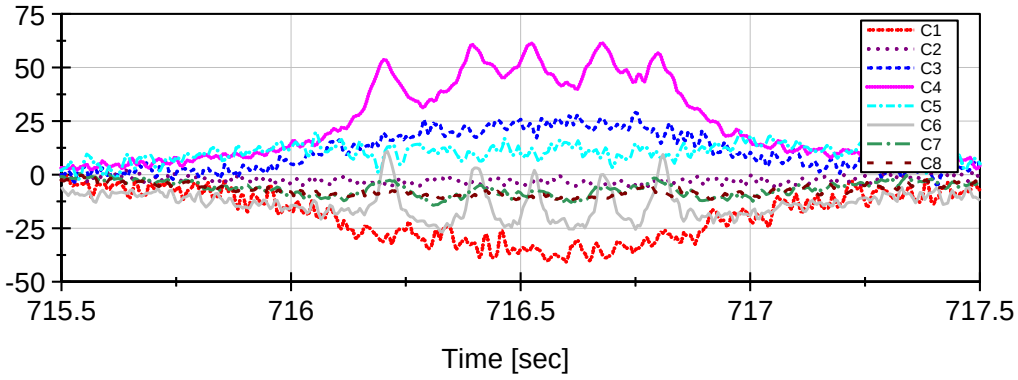

Figure B.6. Strain on concrete during Test 4.

Test 5

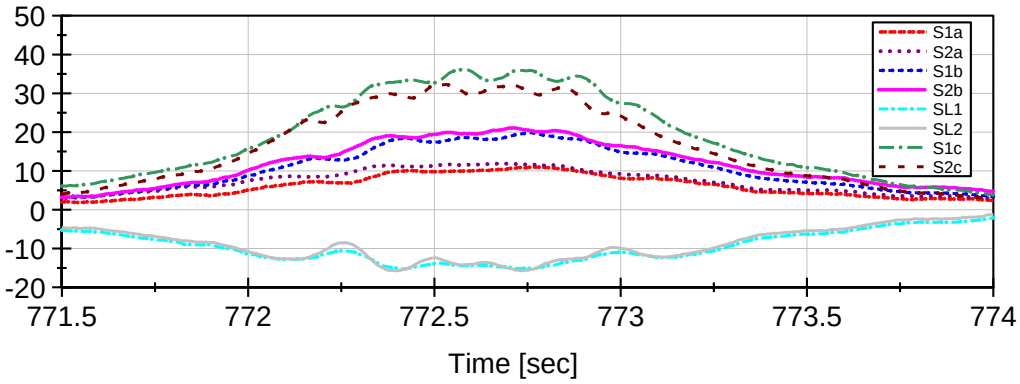

Figure B.7. Strain on rebars during Test 5.

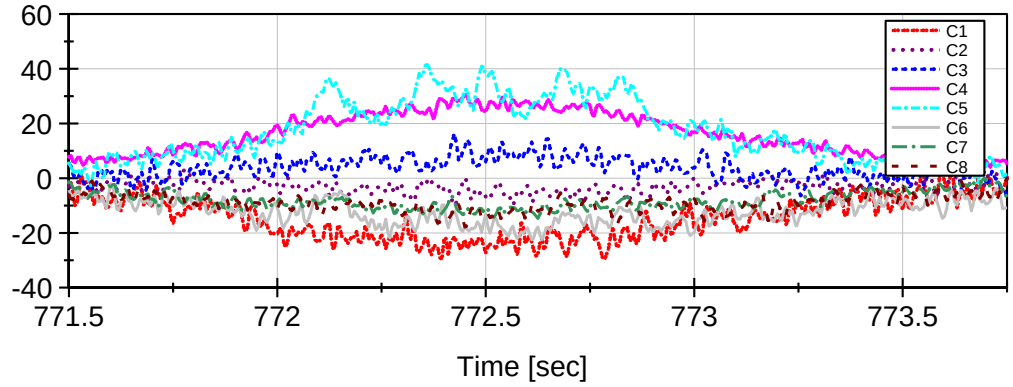

Figure B.8. Strain on concrete during Test 5.

Test 6

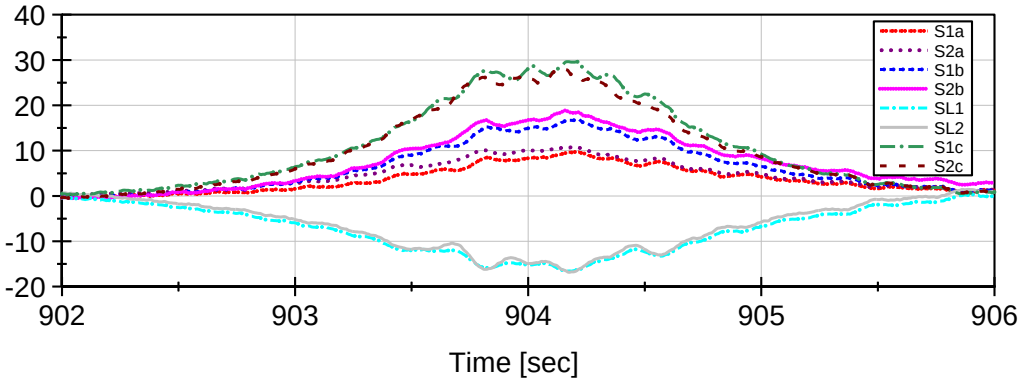

Figure B.9. Strain on rebars during Test 6.

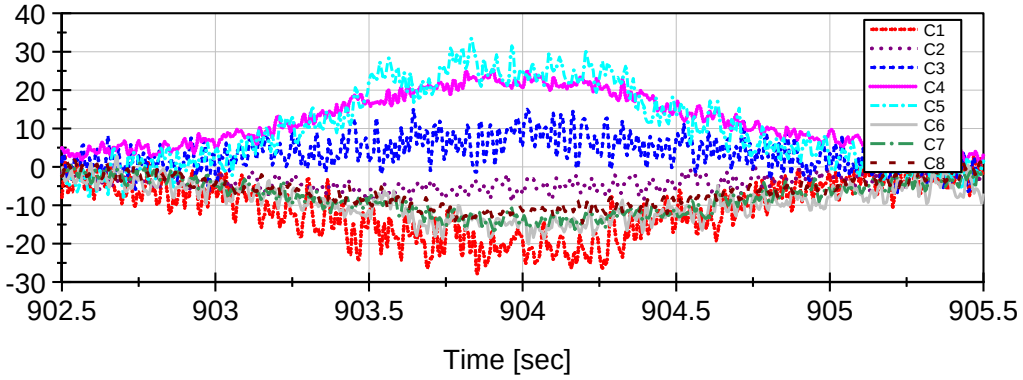

Figure B.10. Strain on concrete during Test 6.

Test 7

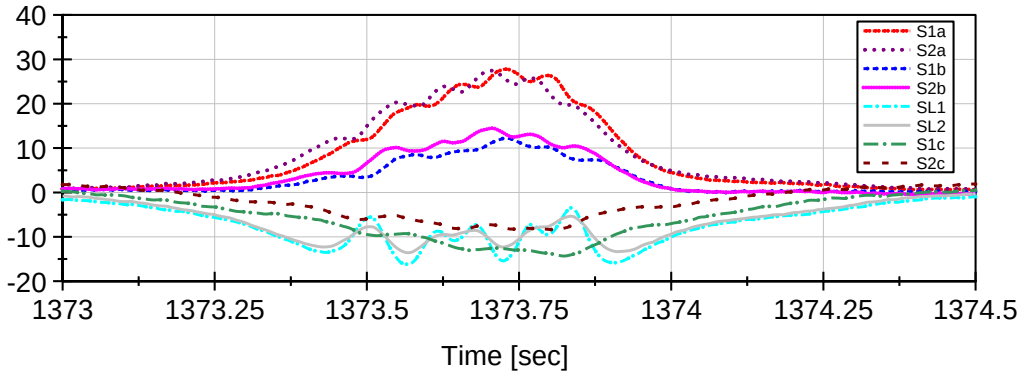

Figure B.11. Strain on rebars during Test 7.

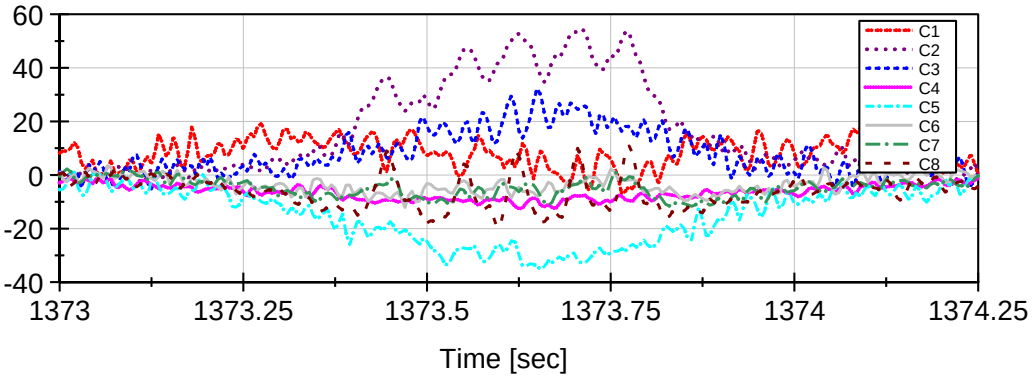

Figure B.12. Strain on concrete during Test 7.

Test 8

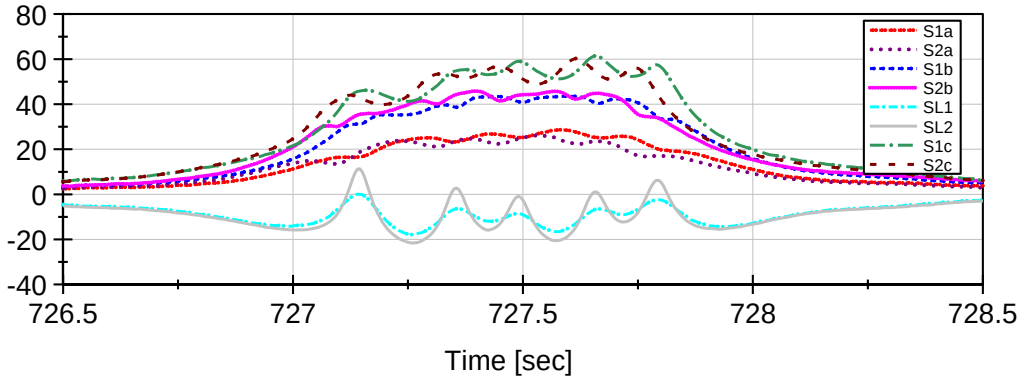

Figure B.13. Strain on rebars during Test 8.

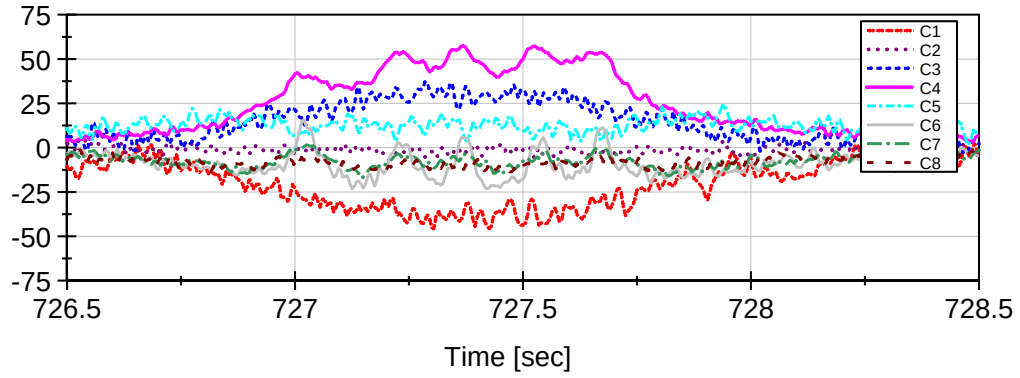

Figure B.14. Strain on concrete during Test 8.

Test 9

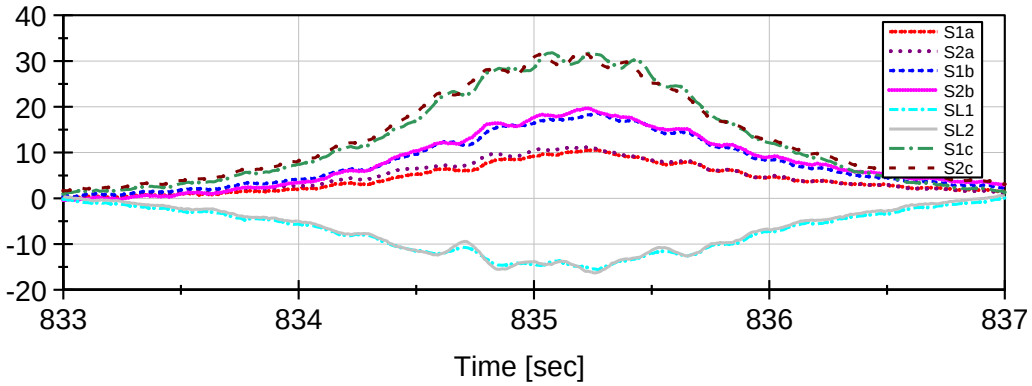

Figure B.15. Strain on rebars during Test 9.

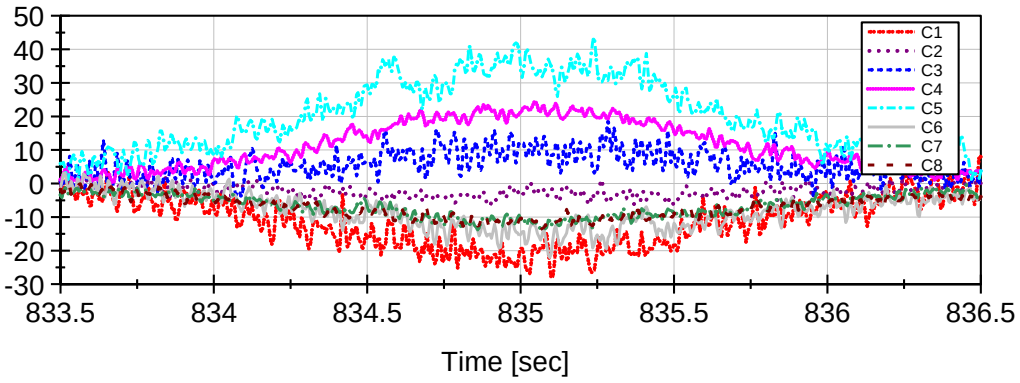

Figure B.16. Strain on concrete during Test 9.

Appendix C – Mid-span reinforcement cross section

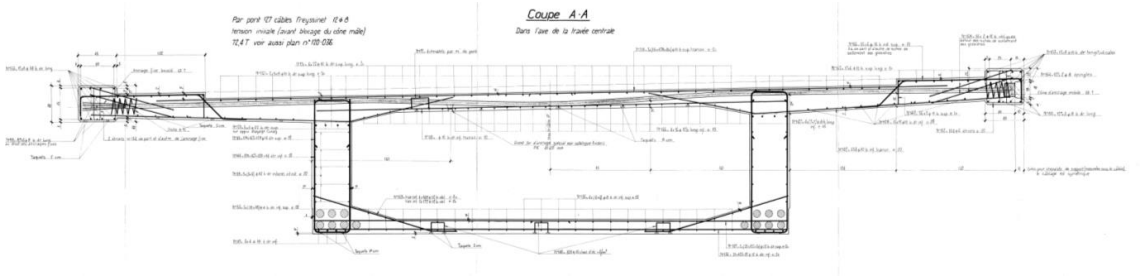

Figure C.1. Transverse section of reinforcement at mid-span.

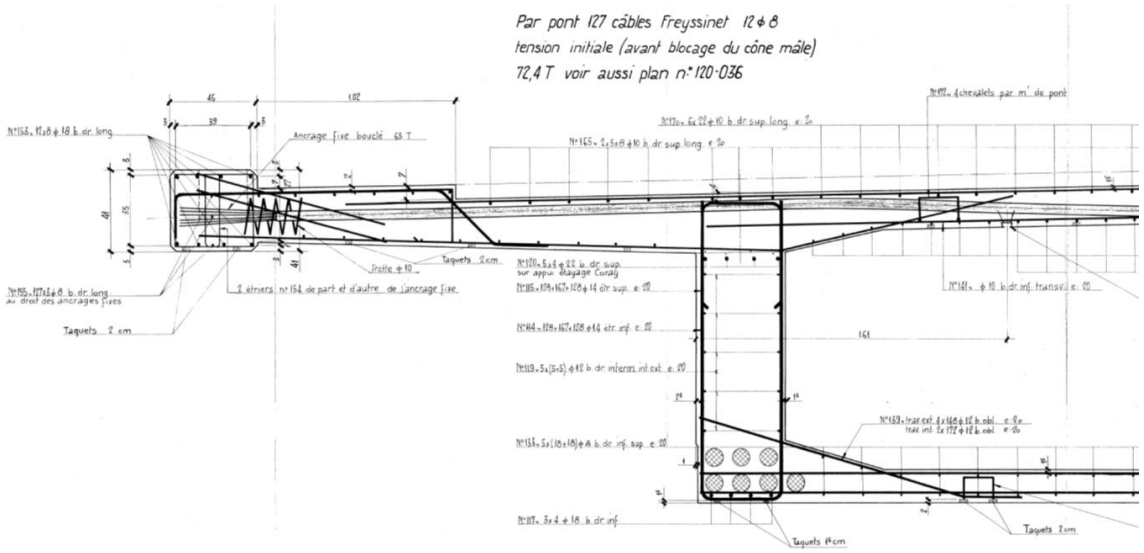

Figure C.2. Transverse section of reinforcement at mid-span (Zoom of left hand side).

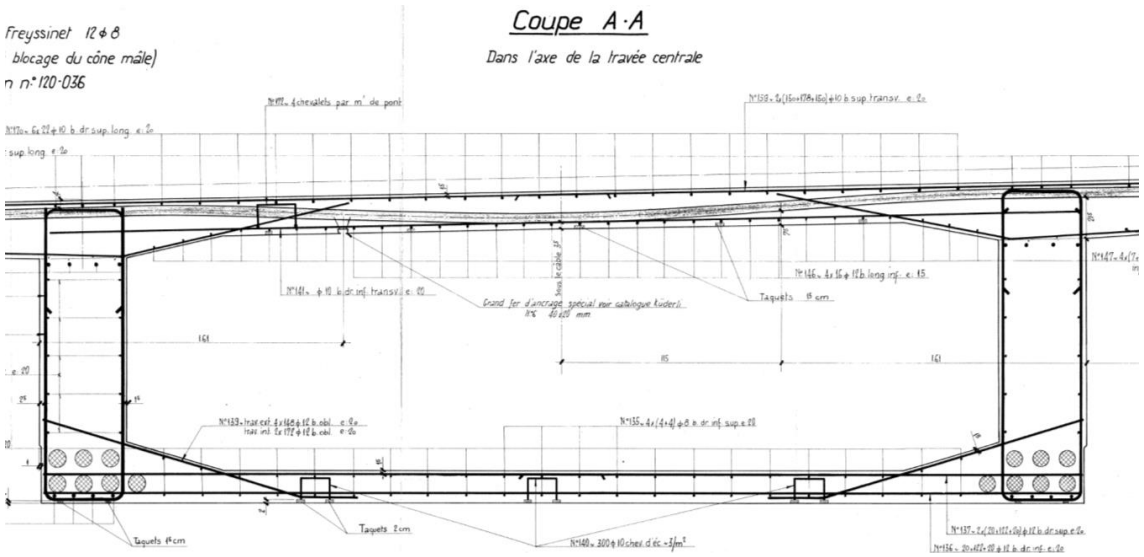

Figure C.2. Transverse section of reinforcement at mid-span (Zoom of centre).

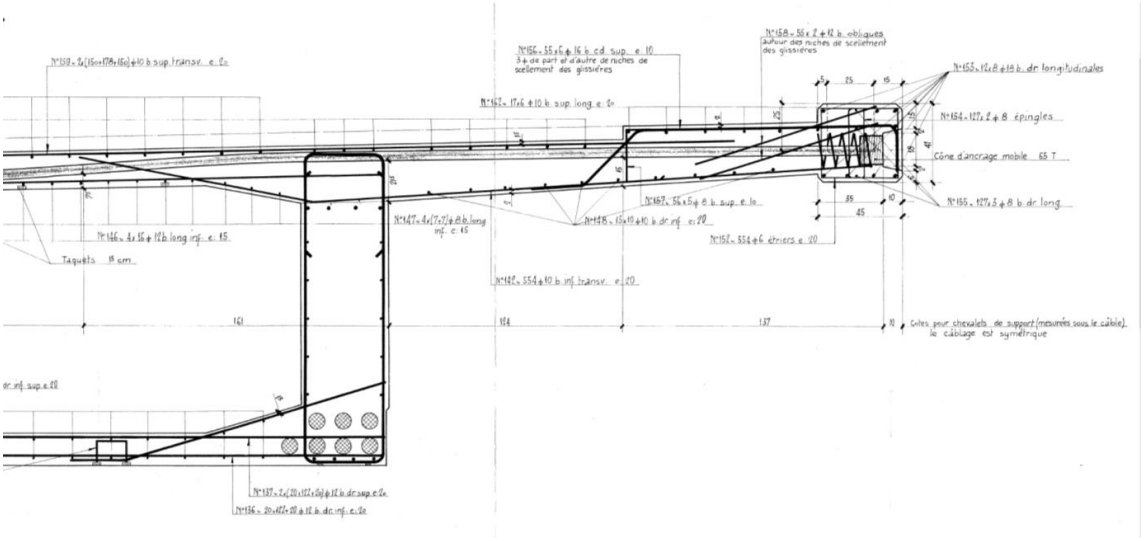

Figure C.3. Transverse section of reinforcement at mid-span (Zoom of right hand side).

Appendix D – Sensor technical details

Table D.1. Strain gauge technical details.

Gauge description	**Steel bar strain gauge**	**Concrete strain gauge**
Ref no:	HBM 1-LY41-100/120	HBM 1-LY61-3/350
Resistance	120Ω ±0.3%	350Ω ±0.3%
k-Factor	2.08 ±1%	2.02 ±1%
Transverse sensitivity	-0.10%	0.20%
Temp co-efficient of gauge factor	93 ±10 [10^{-6}/°C] (-10…+45°c)	93 ±10 [10^{-6}/°C] (-10…+45°c)
Steel with co-eff of thermal expansion, α	10.8 [10^{-6}/°C]	10.8 [10^{-6}/°C]

Table D.2. Accelerometer gauge technical details (HBM).

Type		B12	
Measured quality		constant and varying acceleration, vibration acceleration	
Direction of measurement		selectively along the body axis, anywhere in the field of gravity	
Mechanical principle of measurement		subcritical mechanical oscillating	
Types		B12/200	B12/500
Characteristic frequency appr.	Hz	200	500
Working frequency range	Hz	0...100	0...250
Damping factor D at reference temperature		0.6 ± 0,1	
Nominal acceleration	m/s^2	± 200	± 1000
Sensitivity	mV/V	± 80	± 80
Sensitivity tolerance	mV/V	8	
Nominal sensitivity	mV/V	80	80
Nominal output signal span	mV/V	160	160
Temperature effect per 10K in the nominal temperature range on the sensitivity*), related to the actual value, typ.	%	0.2	
on the zero signal, related of the nominal sensitivity, typ.	%	± 0.25	± 0.25
Linearity deviatation inclusive hysreresis related to the nominal output signal span	%	± 2	
Lateral sensitivity**) (direction factor)	%	± 3	
Relative lateral force limit related to the nominal acceleration	%	± 100	
Electrical principle		ind. system with differential chokes	

*) The characteristic value is the actual output signal at nominal acceleration

**) The lateral sensitivity is the output signal when loaded perpendicular to the measuring axis, referred to the output signal for the same load along the measuring axis of the accelerometer

Types		B12/200	B12/500
Nominal excitation voltage (r.m.s)	V	2.5 ± 5%	
Operating range of the excitation voltage (r.m.s)	V	1...6	
Carrier frequency	kHz	5	
Input resistance at reference temperature (between points 2 and 3)		ca. 40	
Input inductance at reference temperature (between points 2 and 3)	mH	ca. 10	
Reference temperature	°C	+23	
Nominal temperature range	°C	–10... +60	
Operating temperature range	°C	–10... +60	
Storage temperature range	°C	–10... +60	
Weight	g	ca. 17	
Mounting		M6 screw stud	